Biochimica et Biophysica Acta 1837 (2014) 1063–1068

Contents lists available at ScienceDirect

Biochimica et Biophysica Acta

journal homepage: www.elsevier.com/locate/bbabio

Review

Half channels mediating H^+ transport and the mechanism of gating in the F_o sector of *Escherichia coli* F_1F_o ATP synthase☆

Robert H. Fillingame *, P. Ryan Steed

Department of Biomolecular Chemistry, University of Wisconsin School Medicine & Public Health, 420 Henry Mall, Madison, WI 53706-1532, USA

ARTICLE INFO

Article history:
Received 16 December 2013
Received in revised form 6 March 2014
Accepted 10 March 2014
Available online 17 March 2014

Keywords:
F_1F_o ATP synthase
Proton transport
F_o half channels
Gating mechanisms
Trans-membrane helices
Interactions subunits *a* and *c*

ABSTRACT

H^+-transporting F_1F_o ATP synthase catalyzes the synthesis of ATP via coupled rotary motors within F_o and F_1. H^+ transport at the subunit *a*–*c* interface in trans-membranous F_o drives rotation of the *c*-ring within the membrane, with subunit *c* being bound in a complex with the γ and ε subunits extending from the membrane. Finally, the rotation of subunit γ within the $\alpha_3\beta_3$ sector of F_1 mechanically drives ATP synthesis within the catalytic sites. In this review, we propose and provide evidence supporting the route of proton transfer via half channels from one side of the membrane to the other, and the mechanism of gating H^+ binding to and release from Asp61 of subunit *c*, via conformational movements of Arg210 in subunit *a*. We propose that protons are gated from the inside of a four-helix bundle at the periplasmic side of subunit *a* to drive protonation of *c*Asp61, and that this gating movement is facilitated by the swiveling of trans-membrane helices (TMHs) 4 and 5 at the site of interaction with *c*Asp61 on the periphery of the *c*-ring. Proton release to the cytoplasmic half channel is facilitated by the movement of *a*Arg210 as a consequence of this proposed helical swiveling. Finally, release from the cytoplasmic half channel is mediated by residues in a complex of interacting extra-membraneous loops formed between TMHs of both subunits *a* and *c*. This article is part of a Special Issue entitled: 18th European Bioenergetic Conference.

1. Introduction

The F_1F_o-ATP synthase of oxidative phosphorylation utilizes the energy of a trans-membrane electrochemical gradient of H^+ or Na^+ to mechanically drive the synthesis of ATP via two coupled rotary motors in the F_1 and F_o sectors of the enzyme (ref. [1] and Fig. 1). H^+ transport through the transmembrane F_o sector is coupled to ATP synthesis or hydrolysis in the F_1 sector at the surface of the membrane. Homologous ATP synthases are found in mitochondria, chloroplasts, and many bacteria. In *Escherichia coli* and other eubacteria, F_1 consists of five subunits in an $\alpha_3\beta_3\gamma\delta\varepsilon$ stoichiometry. F_o is composed of three subunits in a likely ratio of $a_1b_2c_{10}$ in *E. coli* and *Bacillus* PS3 [2,3] or $a_1b_2c_{11}$ in the Na^+ translocating *Ilyobacter tartaricus* ATP synthase [1,4] and may contain as many as 15 *c* subunits in other bacterial species [5].

Subunit *c* spans the membrane as a hairpin of two α-helices with the first TMH[1] on the inside and the second TMH on the outside of the *c* ring [1,4]. The binding of Na^+ or H^+ occurs at an essential, membrane embedded Glu or Asp on *c*TMH2. A high resolution X-ray structure of the *I. tartaricus* c_{11}-ring revealed a Na^+ binding Glu at the periphery of the ring with chelating groups to the bound Na^+ extending from two adjacent subunits in an extensive hydrogen bonding network [1,4,6]. A high resolution X-ray structure of the H^+-translocating c_{15}-ring of *Spirulina platensis* revealed a similar geometry for the H^+ binding site [5,7]. Several other neighboring residues form a hydrogen bonding network between TMHs 1 and 2 of one subunit and TMH2 from the adjacent subunit. In slight contrast, a recent structure of the c_{13} ring from *Bacillus pseudofirmus* OF4 [8] revealed a more hydrophobic H^+ binding site in which a water molecule is coordinated by the H^+-binding Glu and the backbone of the adjacent *c*TMH2. This H^+ binding mode is likely to also be found in *E. coli* subunit *c*, given the lack of hydrogen bonding side chains surrounding the Asp61 H^+-binding site. In the H^+-translocating *E. coli* enzyme, Asp-61 at the center of *c*TMH2 is thought to undergo protonation and deprotonation as each subunit of the *c* ring moves past the stationary subunit *a*. In the functioning enzyme, the rotation of the *c* ring is proposed to be driven by H^+ transport at the subunit *a*/*c* interface. Subunit γ physically binds to the cytoplasmic surface of the *c*-ring, which results in the coupling of *c*-ring rotation with rotation of subunit γ within the $\alpha_3\beta_3$ hexamer of F_1. The rotation of subunit γ then forces conformational changes in the catalytic sites at αβ subunit interfaces that lead to synthesis of ATP (reviewed in ref. [1]).

E. coli subunit *a* folds in the membrane with five TMHs and is thought to provide aqueous access channels to the H^+-binding Asp-61 residue in the *c*-ring [9,10]. Interaction of the conserved Arg-210 residue in *a*TMH4 with *c*TMH2 is thought to be critical during the deprotonation–protonation cycle of *c*Asp-61 [1,11,12]. Presently, only fragmentary

Abbreviations: N-side, the electrochemically negative side of the membrane; P-side, the electrochemically positive side of the membrane; TM, trans-membrane; TMH, trans-membrane helix; NEM, N-ethylmaleimide

☆ This article is part of a Special Issue entitled: 18th European Bioenergetic Conference.

* Corresponding author. Tel.: +1 608 262 1439; fax: +1 608 262 5253.
E-mail address: rhfillin@wisc.edu (R.H. Fillingame).

http://dx.doi.org/10.1016/j.bbabio.2014.03.005
0005-2728/

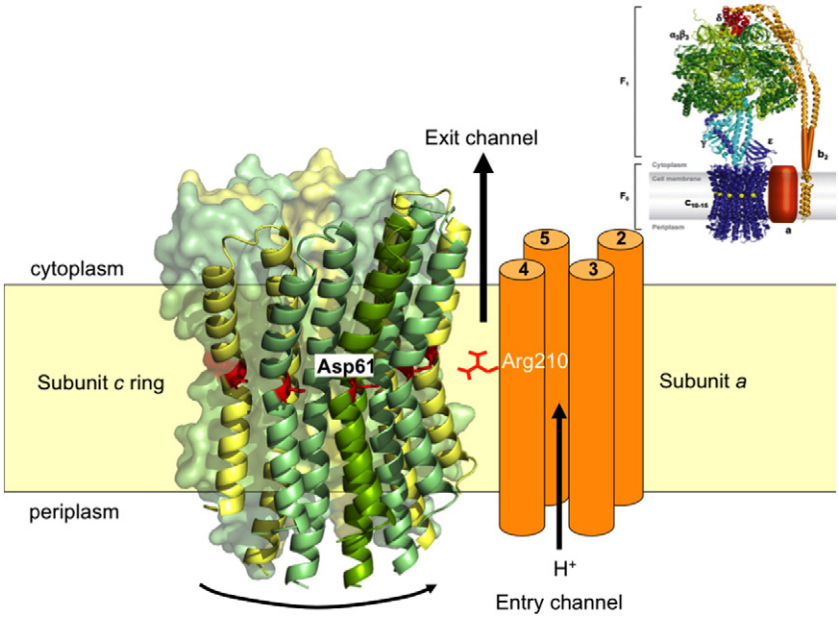

Fig. 1. H^+-transporting F_1F_o ATP synthase catalyzes the synthesis of ATP via coupled rotary motors within F_o and F_1. H^+ transport at the subunit *a*–*c* interface in F_o drives rotation of the *c*-ring-γ–ε complex, and rotation of subunit γ within the $\alpha_3\beta_3$ sector of F_1 then mechanically drives ATP synthesis within the catalytic sites. In this review, we propose the route of proton transfer via two separate half-channels extending from the periplasmic (P) or cytoplasmic (N) sides of the membrane to *c*Asp61 at the center of the membrane. The half channels are gated with the H^+ binding to and release from *c*Asp61 being coupled to conformational movements of Arg210 in subunit *a*. The structural model of F_1F_o shown is reproduced from ref. [1] with permission, and the structural model for the *E. coli* c_{10} ring is that predicted from the X-ray structure of the *I tartaricus* *c*-ring [4,26].

information is available on the three-dimensional arrangement of the TMHs in subunit *a*. TMHs 2–5 of subunit *a* pack in a four-helix bundle, which was initially defined by cross-linking ([13]; Fig. 2), but now such a bundle, packing at the periphery of the *c*-ring, has been viewed directly by high resolution cryo-electron microscopy in the *I. tartaricus* enzyme [14]. Previously published cross-linking experiments support the identification of *a*TMH4 and *a*TMH5 packing at the periphery of the *c*-ring and the identification of *a*THM2 and *a*TMH3 as the other components of the four helix bundle seen in these images [13,15,16]. More recently published cross-linking experiments identify the N-terminal α-helices of two b subunits, one of which packs at one surface of *a*TMH2 with close enough proximity to the *c*-ring to permit

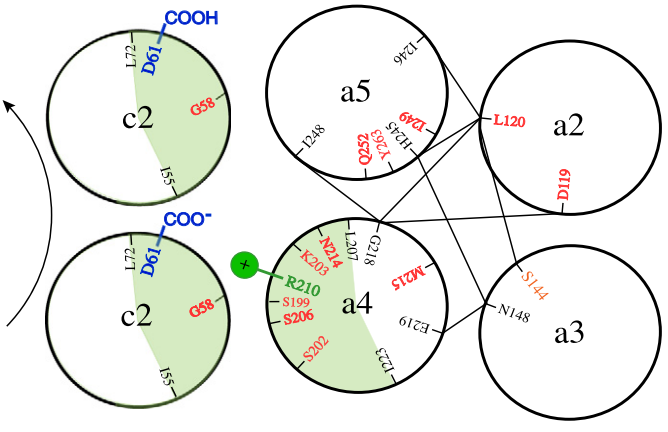

Fig. 2. The predicted cross-sectional packing of TMHs 2–4 of subunit *a* into a four helix bundle and the predicted faces of helix–helix interaction with the peripheral helices of the *c*-ring as viewed from the cytoplasm. The eight cross-links formed in high yield between pairs of Cys introduced into different TMHs of subunit *a* are indicated by the lines between the cross-linkable residues [13]. The predicted packing of TMH2 of subunit *c* with TMHs 4 and 5 of subunit *a* is also based upon Cys–Cys cross-linking [15,16]. Arrows indicate the direction of *c*-ring rotation during ATP synthesis. This figure is modified from that shown in ref. [32].

cross-linking [17]. The other subunit *b* N-terminal helix packs on the opposite peripheral surface of *a*TMH2 in a position where it can also be cross-linked to *a*TMH3 [17]. The N-terminal helix of subunit *b* (residues 1–34) appears to play an important structural role in formation of a functional F_0 [18]. The last helix density shown in Hakulinen *et al.* [14] packs at the periphery of the *c*-ring next to *a*TMH5 and is very likely to be *a*TMH1. If *a*TMH1 is packing at this position, the long cytoplasmic 1-2 loop must extend across *a*TMH5 before reaching *a*TMH2 (see Fig. 3).

Cross-linking experiments have also defined the juxtaposition of *a*TMH4 and *c*TMH2 over a span of 19 amino acids, a span that would nearly traverse the lipid bilayer [15]. The cross-linkable faces of these helices would include Asp-61 in *c*TMH2 and residues of *a*TMH4 surrounding the conserved Arg-210. Cross-linking experiments have also established the close packing proximity of *a*TMH5 and *c*TMH2 from the center of the lipid bilayer to the cytoplasmic surface of the membrane [16]. The cross-linkable face of *a*TMH5 includes Gln252, which has been proposed to be proximal to Arg210 because of retention of function in *a*R210/Q252R second site suppressor mutants [19,20]. The importance of precise vertical positioning of the interacting residues was addressed by Langemeyer and Engelbrecht [21].

The aqueous accessibility of Cys residues introduced into the 5 TMHs of subunit *a* has been probed based upon their reactivity with and inhibitory effects of Ag^+ and other thiolate-reactive agents [22–24]. Two regions of aqueous access were found with distinctly different properties. One region in TMH4, extending from Asn-214 and Arg-210 at the center of the membrane to the cytoplasmic surface, contains Cys substitutions that are sensitive to inhibition by both NEM and Ag^+ ([22–24]; Fig. 3). These NEM and Ag^+ sensitive residues in TMH4 pack at or near the peripheral face and cytoplasmic side of the modeled four-helix bundle [11,13]. The route of aqueous access to the cytoplasmic side of subunit *c* packing at the *a*–*c* interface has also been mapped by the chemical probing of Cys substitutions and more recently by molecular dynamic simulations ([25–27]; Fig. 2).

A second set of Ag^+-sensitive substitutions in subunit *a* mapped to the opposite face and periplasmic side of *a*TMH4 [22,23], and Ag^+-sensitive substitutions were also found in TMHs 2, 3, and 5 where

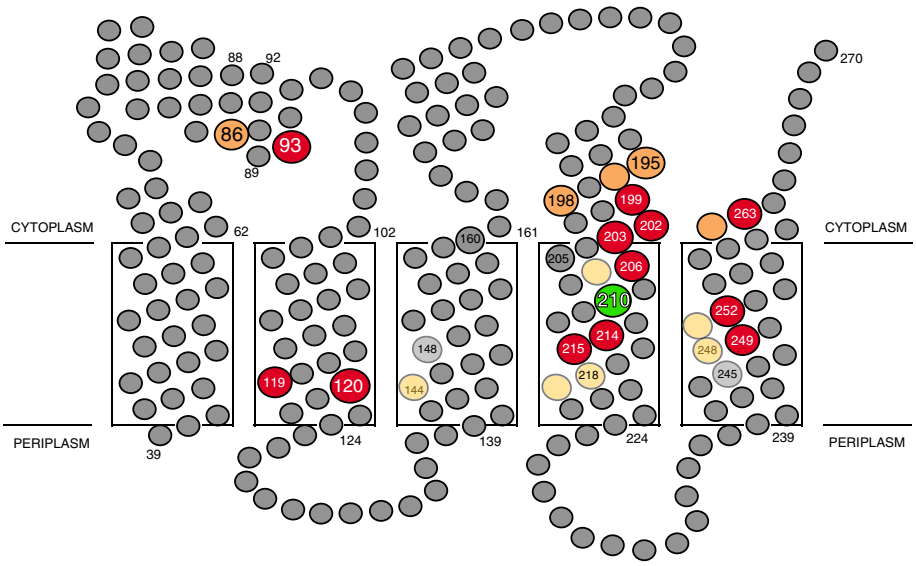

Fig. 3. The predicted topology of subunit *a* in the *E. coli* inner membrane with location of the most Ag^{+}-sensitive Cys substitutions highlighted in *red* (>85% inhibition) and some of the more moderately sensitive residues highlighted in *orange* (66–85% inhibition). The numbered residues are discussed elsewhere in the text. TMHs 1–5 are shown in boxes within the lipid bilayer. Periplasmic loops 1–2 and 3–4 extend from the C-terminal end of TMH1 to the N-terminal end of TMH2, or from the C-terminal end of TMH3 to the N-terminal end of TMH4, respectively. This figure is modified from that shown in ref. [34].

they extend from the center of the membrane to the periplasmic surface ([23,24]; see Figs. 2 & 3). The Ag^{+}-sensitive substitutions on the periplasmic side of TMHs 2–5 cluster at the interior of the four-helix bundle predicted by cross-linking (Fig. 2), and could interact to form a continuous aqueous pathway extending from the periplasmic surface to the central region of the lipid bilayer [11,13,23,24].

The experiments described in the sections below, focus mainly on work done in our own lab over the last decade. Together with work from other labs, the experiments suggest a stepwise pathway/route of proton movement through the F_o sector of the ATP synthase including: (1) proton movement from the periplasmic (P-side) of the inner membrane to the center of the membrane's lipid bilayer via residues centered in the four helix bundle within subunit *a*; (2) the gating of movement of a single proton from the periplasmic half channel to *c*Asp61 via swiveling of TMHs at the *a*–*c* subunit interface; (3) the release of the proton from *c*Asp61 into a cytoplasmic half channel at the interface of the *a* and *c* subunits; and finally, (4) the gating of proton release at the cytoplasmic (N-side) of the membrane via residues in interacting cytoplasmic loops connecting TMHs within both the *a* and *c* subunits. The movement of a single proton across the membrane via the four steps listed above is expected to result in the ratcheted rotation of the *c*-ring by 36°, a prediction that is now experimentally verified [28–30], with a total of ten such ratcheted steps being required for complete rotation of the *c*-ring.

2. Periplasmic channel at the center of a four helix bundle within subunit *a*

Sites of interaction of the TMHs of subunit *a* were defined by zero-length cross-linking with pairs of Cys introduced into different TMHs [13]. The initial regions of interaction tested were those suggested by second site suppressor mutations that restore function to the primary mutants. Eight of the 84 double Cys pairs constructed formed high yield cross-links, and these high yield cross-linkable pairs are represented in Fig. 2. The proximities of interaction agree well with the position of second site suppressor pairs, i.e. residue 218 (TMH4) with residue 245 (TMH5), residue 219 (TMH4) with residue 145 (TMH3), and residue 245 (TMH5) with residue 119 (TMH2) respectively [9,31]. The Cys substitutions at the periplasmic side of subunit *a* that proved to be most sensitive to inhibition by Ag^{+} are located at the interior of this proposed 4 helix bundle (Fig. 2). The Ag^{+} sensitivity of the Cys substitutions at the interior of the four helix bundle indicated aqueous access to this region, but did not prove that access was from the periplasm. A subsequent study testing the Cd^{+2} sensitivity of these residues did prove that the aqueous access pathway was from the periplasm. In contrast to Ag^{+}, Cd^{+2} proves to be membrane impermeant, and when inside-out inner membrane vesicles were treated with Cd^{+2}, the Cys substitutions subject to inhibition all mapped to the cytoplasmic side of the membrane (ref. [32] and see Fig. 3). However, when membrane vesicles from Cys substitutions at positions 119, 120, 214, 215 and 252 were sonically disrupted during Cd^{+2} treatment to permit Cd^{+2} access to the interior of the vesicle, the ATP-driven proton translocation activity was inhibited. The accessibility of the N214C and Q252C substitutions from the periplasm is particularly notable since both residues must also have access to a region around Asp61 for reasons described in the following section.

3. TM helix swiveling and the gating of H^{+} from the periplasmic half channel to *c*Asp61

We have proposed that *a*TMHs 4 and 5 may swivel or twist in response to acidification of the periplasmic half-channel in the TMH 2–5 four-helix bundle, and in so doing gate entry of one H^{+} into the cytoplasmic half-channel with a subsequent protonation of *c*Asp61 [16]. The suggestion was provoked by experiments where cross-link formation between three specific pairs of Cys substitutions in *a*TMH5 and *c*TMH2 was promoted by decreasing the buffering pH (ref. [16]). The ionized Cys thiolate is the reactive group in these reactions and one would therefore expect that cross-linking should decrease with acidification of the medium. The position of the Cys pairs undergoing H^{+}-promoted cross-linking is shown in Fig. 4; acid-promoted cross-linking was not seen in the case of 10 other cross-linkable *a*TMH5/*c*TMH2 Cys pairs. On visualizing Fig. 4, it is apparent that the turning of *a*TMH5 in a clock-wise direction should bring *a*Y263C and *a*Q252C closer to the Cys residues to which they cross-link in *c*TMH2.

To test whether TM helical movement, perhaps swiveling, was necessary during F_1F_o function, we cross-linked *a*TMH2 or *a*TMH4 to *a*TMH5 via Cys substitutions locating to the middle of the lipid bilayer and then tested for function. The cross-linking of the Cys pairs *a*G218C (TMH4) and *a*I248C (TMH5), or *a*L120C (TMH2) and *a*H245C (TMH5),

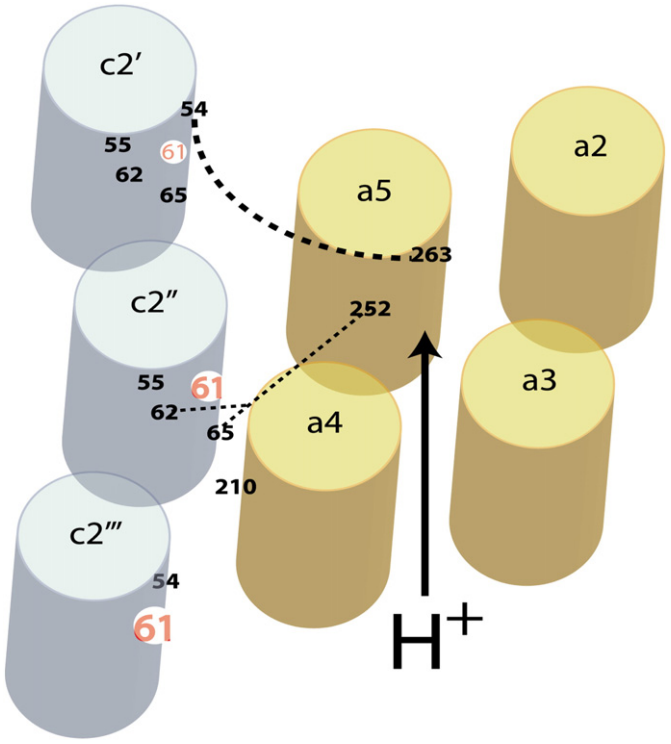

Fig. 4. Acidification of the periplasmic half channel centered in the four helix bundle of subunit *a* is predicted to promote helical swiveling of TMHs 4 and 5 to facilitate cross-linking of Cys252 and Cys263 in *a*TMH5 with Cys substitutions on the peripheral face of the *c*-ring [16]. The *a*Cys263–*c*Cys54 and *a*Cys252–*c*Cys62/65 cross-links are indicated by dashed lines. This figure was drawn by Dr. Kyle Moore, the lead author of the reference cited here [16].

inhibited H^+ pumping by 85–90% and support the idea that mobility of the helices is required for function [33]. H^+ pumping function was largely unaffected by the identical chemical modification of the same Cys residues in the absence of cross-link formation. In additional control experiments, we assessed the effects on function of Cys–Cys cross-linking in other regions of the protein. As is discussed below, the cytoplasmic loops of subunit *a* had previously been implicated in gating H^+ release to the cytoplasm, and previous Cys–Cys cross-linking experiments indicated that the chemically reactive regions of the loops packed together as a single domain [34]. In these cases, Cys substitutions in these domains could be cross-linked with retention of function and hence any conformational movements, which would be restricted by these cross-linking reactions, are not necessary for function in at these domains of the enzyme. In summary, the inhibition observed on cross-linking Cys within TM regions is consistent with the proposed requirement for TMH movements during the gating of periplasmic H^+ access to *c*Asp61. This movement is presumed to be related to the movement of *a*Arg210 away from *c*Asp61 to allow its protonation on gating access of one proton from the periplasmic half channel.

We suggest here that the swiveling of *a*TMH4 in the counter-clockwise direction and *a*TMH5 in the clockwise direction moves N214 in TMH4 and Gln252 in TMH5 to a position close to *c*Asp61 and provides a conduit for a H^+ within the periplasmic half channel to access and protonate the ionized *c*Asp61 residue. We also propose that the protonation of ionized *c*Asp61 would be facilitated by the breaking of the salt bridge with *a*Arg210, which would be forced by the H^+-driven counter-clockwise swiveling of *a*TMH4. In addition, we propose that the H^+ binding site within the periplasmic channel likely involves the interaction of *a*H245 and *a*D119 side-chains. The His side-chain requirement is supported by the need for second site suppression of the *a*H245C substitution by the *a*D119H mutation for functional activity [9]. And, as likened to a ratchet tool, the swiveling must be reversed back to the original positions for the next gating event to occur.

4. Release of H^+ from *c*Asp61 into the cytoplasmic half channel

We propose that the release of H^+ from the protonated *c*Asp61 occurs concurrently with the closure of the H^+ gate of protons from the periplasmic half channel by the reversed helical swiveling of *a*TMH4 and *a*TMH5. These movements would take place concurrently with the rotation of the *c*-ring and a new *a*Arg210/*c*Asp61 salt bridge would form at the position of the *c*Asp61 that has just undergone deprotonation with release of H^+ to the cytoplasmic half-channel. The H^+ released into the cytoplasmic half-channel would flow to the cytoplasmic side of the membrane via an aqueous access pathway defined by the Ag^+-sensitive residues at this side of the membrane in subunit *c* and the interacting face of *a*TMH4 (Figs. 3 and 5). In Fig. 5, the Ag^+ sensitive residues surrounding Asp61 include residues that are oriented towards *c*TMH1. A recent crystal structure of the yeast *c*-ring revealed inter-helical water molecules at this interface [35]. Such aqueous penetration, at least when the binding site is in the open state, may explain the Ag^+ sensitivity, where the Ag^+ likely finds access after dissolving in the membrane as described in ref. [22]. The much more limited access of the membrane impermeant Cd^{+2} to these residues provides further support for the idea that the H^+ exit pathway to the cytoplasm is

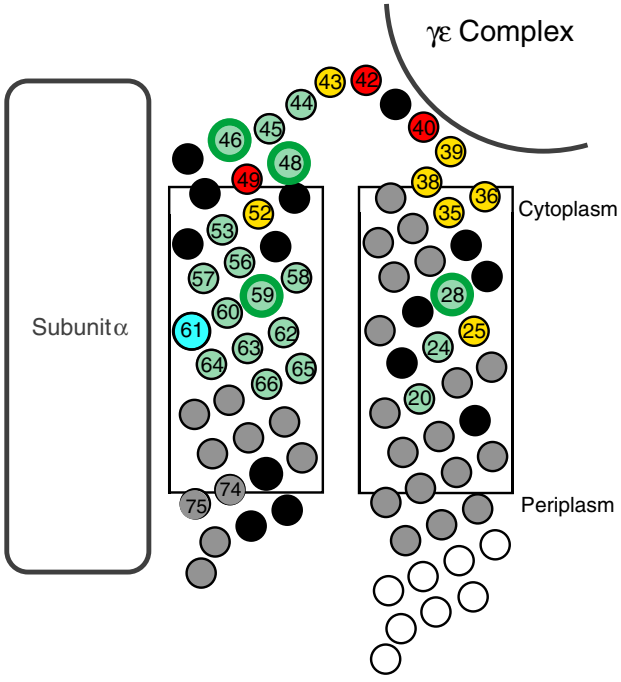

Fig. 5. Functionally distinct regions of metal sensitive residues in the polar loop of subunit *c*. The TMHs of subunit *c* are shown in boxes extending from the periplasmic side to the cytoplasmic side of the lipid bilayer. Ag^+-sensitive Cys residues that are thought to be aqueous accessible are colored *green*. In these cases, Ag^+ inhibition is reversed by dithiothreitol treatment by at least 75%. The residues highlighted with *dark green* circles were shown to directly mediate passive H^+ translocation through F_o. The Cys residues in *red* are thought to be involved in the binding and coupling of F_1 to F_o, and in these cases, Ag^+ treatment causes disassociation of F_1 from the membrane and hence inhibition of activity is not reversed by dithiothreitol treatment. The mechanism of Ag^+ inhibition of Cys substitutions that are colored *yellow* is less certain as these substitutions exhibit some properties consistent with uncoupling of F_1 from F_o and Ag^+ inhibition is only partially reversed by dithiothreitol. The Cys substitutions at the positions colored in *black* are not active, as is the case for the D61C substitution (*cyan*). The Cys substitutions colored in *grey* are relatively insensitive to Ag^+ treatment, and Cys replacements have not been made in the residues depicted in *white*. The Cys substitutions at positions 74 and 75 are thought to form cross-links with Cys in the neighboring subunit *c* in response to Ag^+ treatment with a resultant inhibition of function [36]. The figure shown is modified from that depicted in ref. [36].

primarily at the *a*–*c* interface, i.e., the only TM Cys that are sensitive to Cd^{+2} are at positions 28 in TMH1 and 57–59 and 63 in TMH2 [26]. The aqueous pathway from the cytoplasm includes three Cys substitutions that are uniquely sensitive to inhibition by N-ethylmaleimide (NEM), i.e. the G58C substitution in subunit *c* and the S206C and N214C substitutions in subunit *a* [22,25,26]. These are the only NEM-sensitive Cys substitutions in subunits *a* and *c*, which suggests that they lie in a chemically unique cavity surrounding the *c*Asp61 carboxylate. When we recall that the *a*N214C substitution is also accessible to Cd^{+2} [32], but only from the periplasm, it further fortifies the role of this residue in gating H^+ movement to *c*Asp61 from the periplasmic half-channel to the cytoplasmic half- channel.

5. H^+ gating to the cytoplasm via interacting extra-membranous loops of subunits *a* and *c*

The exit of H^+ to the cytoplasmic side (N-side) of the inner membrane utilizes a channel at the interacting faces of *a*TMH4 and *c*TMH2 that continues into cytoplasmic domains extending beyond the surface of the lipid bilayer. The Ag^+-sensitive residues in both the 1-2 loop and the 3-4 loop of subunit *a* appear to be involved in gating H^+ translocation to the cytoplasm ([34]; see Fig. 3), and by experiments that are described below have now been shown to interact with residues in the polar loop region of subunit *c* that is directly implicated in proton translocation. Cys substitutions within the polar loop of subunit *c* are inhibited by two distinct mechanisms upon treatment with Ag^+. For most substitutions in the loop showing moderate to strong inhibition by Ag^+, the Ag^+ treatment resulted in perturbation of the interaction of F_1 with F_o, which was often accompanied with dissociation of F_1 from the membrane [36]. In these cases, the inhibition cannot be reversed by treatment with dithiothreitol, which chelates the Ag^+ bound to the inhibitory Cys substitution. In a second class of Ag^+-sensitive Cys substitutions in the polar loop region, Ag^+ inhibition was largely reversed by dithiothreitol treatment, and this was also true for the trans-membrane Cys substitutions that are thought to line the cytoplasmic H^+ channel within subunit *c* (Fig. 5). In the select cases examined, where the DTT-reversible Cys substitutions were also sensitive to Cd^{+2} inhibition, the treatment with Cd^{+2} was shown by direct assays to inhibit passive H^+ translocation through F_o. In the case of subunit *c*, this was shown not only for TM Cys substitutions (at positions 28 and 59), but also for the Cys46 and Cys 48 substitutions in the polar loop.

The cytoplasmic loops of subunit *a* also appear to directly participate in proton transport and release to the cytoplasm (P. R. Steed, K. Kraft and R. H. Fillingame, *in preparation*). The inhibition of passive H^+ translocation through F_o by Cd^{+2} was directly shown for not only the transmembrane Cys214 substitution, but also for Cys 199 and 202 in the 3-4 loop and Cys263 within the cytoplasmic domain following *a*TMH5. In each of these cases, the inhibitory effects of Cd^{+2} or Ag^+ were fully reversed by DTT. Based upon the criteria of DTT-reversibility, the Ag^+-sensitive but Cd^{+2} insensitive Cys substitutions at positions 93, 195, 196 and 203 are also thought to directly participate in proton translocation. Within subunit *a*, the *a*M93C substitution in the 1-2 cytoplasmic loop was previously shown to cross-link with *a*L195C in the 3-4 loop region and suggested that these Ag^+-sensitive residues interacted in a single domain to gate proton transport to the cytoplasm [34]. This proposed gating domain can now be extended to the polar loop of subunit *c* with the finding that either *c*I46C or *c*L48C can be cross-linked to the *a*M93C substitution in subunit *a* (P. R. Steed, K. Kraft and R. H. Fillingame, *in preparation*). Previous experiments with photo-activatable cross-linkers support the proximity of the 3-4 loop in subunit *a* to cytoplasmically exposed regions of subunit *c* [37].

6. How does H^+-transport driven helical swiveling within subunit *a* drive *c*-ring rotation?

In Fig. 6 we present a schematic model summarizing how helical movements at the subunit *a*/*c*-ring interface might be coupled with the stepwise rotation of the *c*-ring by 36° as each proton is translocated.

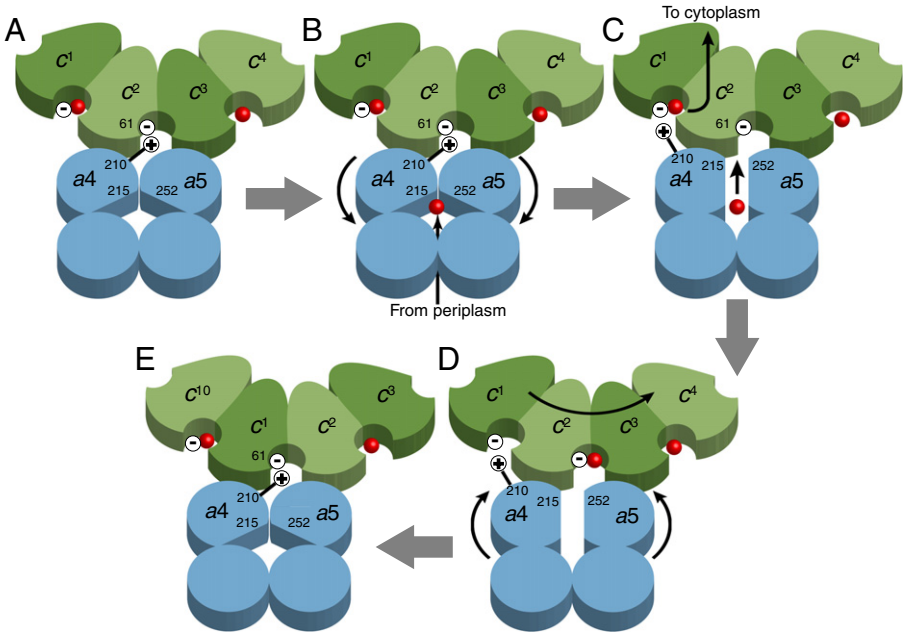

Fig. 6. Schematic model for how changes in TMH interactions at the subunit *a*–*c* interface promote translocation of one H^+ with the coupled stepwise 36° rotational movement of the *c*-ring. The peripheral ring of *c*TMH2's (in *green*), numbered from 1 to 10, is shown packing proximally to TMH4 and TMH5 of subunit *a* (in *cyan*). *A.* Initial state with *a*Arg210 in salt bridge with *c*Asp61 following H^+ exit to the cytoplasm and coupled *c*-ring rotor movement in the previous cycle. *B.* Entry of one H^+ into the periplasmic half channel followed by helical swiveling of *a*TMH4 and *a*TMH5 to gate H^+ access to *c*Asp61. *C.* *a*TMH4 swiveling drives formation of a salt bridge between *a*Arg210 and the *c*Asp61 in counter-clock-wised positioned *c*TMH2 (#1) and release of its bound H^+ to the cytoplasmic half channel, while simultaneously, *c*Asp61 of *c*TMH2 (#2) is protonated from the periplasm. *D.* Swiveling of *a*TMH4 and *a*TMH5 back to their original positions results in the dragging of the *c*-ring in the clockwise direction such that *c*TMH2 (#1) assumes the position of *c*TMH2 (#2) in the initial state. *E.* Final state, equivalent to that in state *A*, after translocation of one H^+ and 36° movement of the *c*-ring rotor.

Some of the amino acid residues participating in each step were at least tentatively identified in Sections 2–5 above. The protonmotive force is thought to drive the initial swiveling of helices in step 2 with consequent translocation of the proton to the cytoplasm. In step 4, the swiveling of *a*TMH4 and *a*TMH5 back to their original position generates sufficient torque to move the *c*-ring by 36° and generates a new set of interactions with the next *c* subunit in the ring and subunit *a* that are comparable to those in the starting state. The key unanswered question relates to how these swiveling movements might generate the torque. We now have multiple estimates of the magnitude of the torque required [30,38], and kinetic measurements showing that the 36° substeps are sufficiently fast such that they should not be rate limiting in either the ATP synthesis or hydrolysis mode [29], given the elasticity of the system [38]. What are the key structural features in the *a*–*c* helical interactions that force movement of the rotor with TMH swiveling? Certainly the *a*Arg210-*c*Asp61 salt bridge could be a key component, but there must be others, with additional salt bridges at the cytoplasmic *a*–*c* interface being suggested to likely be important by others [29]. Ultimately we might expect that future crystal structures will define close packing interactions between the TMHs of *c*TMH2 and TMHs 4 and 5 of subunit *a*. Hopefully, other future crystal structures will show how these packing interactions change in response to changes in pH, as does the rate of select cross-linking reactions between these helices, and give the first structural clues as to how the protonmotive force physically drives *c*-ring rotation. With a single crystal structure, molecular dynamics analyses might provide early insights into the possible changes in packing interactions, which together with thermodynamic analyses might indicate whether the proposed changes in packing provide sufficient torque energy to drive the *c*-ring rotation. We look forward to these future key developments.

Acknowledgment

The research described here was supported by United States Public Health Service Grant GM23105 from the National Institutes of Health.

References

[1] C. von Ballmoos, A. Wiedenmann, P. Dimroth, Essentials for ATP synthesis by F_1-F_O ATP synthases, Annu. Rev. Biochem. 78 (2009) 649–672.
[2] W. Jiang, J. Hermolin, R.H. Fillingame, The preferred stoichiometry of *c* subunits in the rotary motor sector of *Escherichia coli* ATP synthase is ten, Proc. Natl. Acad. Sci. U. S. A. 98 (2001) 4966–4971.
[3] N. Mitome, T. Suzuki, S. Hayashi, M. Yoshida, Thermophilic ATP synthase has a decamer *c*-ring: indication of noninteger 10:3H^+/ATP ratio and permissive elastic coupling, Proc. Natl. Acad. Sci. U. S. A. 101 (2004) 12159–12164.
[4] T. Meier, P. Polzer, K. Diederichs, W. Welte, P. Dimroth, Structure of the rotor ring of F-type Na^+-ATPase from *Ilyobacter tartaricus*, Science 308 (2005) 659–662.
[5] D. Pogoryelov, O. Yildiz, J.D. Faraldo-Gomez, T. Meier, High-resolution structure of the rotor ring of a proton-dependent ATP synthase, Nat. Struct. Mol. Biol. 16 (2009) 1068–1073.
[6] T. Meier, A. Krah, P.J. Bond, D. Pogoryelov, K. Diederichs, J.D. Faraldo-Gomez, Complete ion-coordination structure in the rotor ring of Na^+-dependent F-ATP synthases, J. Mol. Biol. 391 (2009) 498–507.
[7] A. Krah, D. Pogoryelov, J.D. Langer, P.J. Bond, T. Meier, J.D. Faraldo-Gómez, Structural and energetic basis for H(+) versus Na(+) binding selectivity in ATP synthase F(o) rotors, Biochim. Biophys. Acta 1797 (2010) 763–772.
[8] L. Preiss, O. Yildiz, D.B. Hicks, T.A. Krulwich, T. Meier, A new type of proton coordination in an F_1F_O-ATP synthase rotor ring, PLoS Biol. 8 (2010) e1000443.
[9] F.I. Valiyaveetil, R.H. Fillingame, Transmembrane topography of subunit *a* in the *Escherichia coli* F_1F_o ATP synthase, J. Biol. Chem. 273 (1998) 16241–16247.
[10] T. Wada, J.C. Long, D. Zhang, S.B. Vik, A novel labeling approach supports the five-transmembrane model of subunit *a* of the *Escherichia coli* ATP synthase, J. Biol. Chem. 274 (1999) 17353–17357.
[11] R.H. Fillingame, C.M. Angevine, O.Y. Dmitriev, Mechanics of coupling proton movements to *c*-ring rotation in ATP synthase, FEBS Lett. 555 (2003) 29–34.
[12] S.B. Vik, R.R. Ishmukhametov, Structure and function of subunit *a* of the ATP synthase of *Escherichia coli*, J. Bioenerg. Biomembr. 37 (2005) 445–449.
[13] B.E. Schwem, R.H. Fillingame, Cross-linking between helices within subunit *a* of *Escherichia coli* ATP synthase defines the transmembrane packing of a four helix bundle, J. Biol. Chem. 281 (2006) 37861–37867.
[14] J.K. Hakulinen, A.L. Klyszejko, J. Hoffmann, L. Eckhardt-Strelau, B. Brutschy, J. Vonck, T. Meier, Structural study on the architecture of the bacterial ATP synthase F_o motor, Proc. Natl. Acad. Sci. U. S. A. 109 (2012) E2050–E2056.
[15] W. Jiang, R.H. Fillingame, Interacting helical faces of subunits *a* and *c* in the F_1F_o ATP synthase of *Escherichia coli* defined by disulfide cross-linking, Proc. Natl. Acad. Sci. U. S. A. 95 (1998) 6607–6612.
[16] K.J. Moore, R.H. Fillingame, Structural interactions between transmembrane helices 4 and 5 of subunit *a* and the subunit *c* ring of *Escherichia coli* ATP synthase, J. Biol. Chem. 283 (2008) 31726–31735.
[17] J. DeLeon-Rangel, R.R. Ishmukhametov, W. Jiang, R.H. Fillingame, S.B. Vik, Interactions between subunits *a* and *b* in the rotary ATP synthase as determined by cross-linking, FEBS Lett. 587 (2013) 892–897.
[18] J.-C. Greie, T. Heitkamp, K. Altendorf, The transmembrane domain of subunit *b* of *Escherichia coli* F_1F_0 ATP synthase is sufficient for H^+-translocating activity together with subunits *a* and *c*, Eur. J. Biochem. 271 (2004) 3036–3042.
[19] L.P. Hatch, G.B. Cox, S.M. Howitt, The essential arginine residue at position 210 in the *a* subunit of the *Escherichia coli* ATP synthase can be transferred to position 252 with partial retention of activity, J. Biol. Chem. 270 (1995) 29407–29412.
[20] R.R. Ishmukhametov, J.B. Pond, A. Al-Huqail, M.A. Galkin, S.B. Vik, ATP synthesis without R210 of subunit *a* in the *Escherichia coli* ATP synthase, Biochim. Biophys. Acta 1777 (2008) 32–38.
[21] L. Langemeyer, S. Engelbrecht, Essential arginine in subunit *a* and aspartate in subunit *c* of F_oF_1 ATP synthase: Effect of repositioning within helix 4 of subunit *a* and helix 2 of subunit *c*, Biochim. Biophys. Acta 1767 (2007) 998–1005.
[22] C.M. Angevine, R.H. Fillingame, Aqueous access channels in subunit *a* of rotary ATP synthase, J. Biol. Chem. 278 (2003) 6066–6074.
[23] C.M. Angevine, K.A. Herold, R.H. Fillingame, Aqueous access pathways in subunit *a* of rotary ATP synthase extend to both sides of the membrane, Proc. Natl. Acad. Sci. U. S. A. 100 (2003) 13179–13183.
[24] C.M. Angevine, K.A. Herold, O.D. Vincent, R.H. Fillingame, Aqueous access pathways in ATP synthase of subunit *a*: reactivity of cysteine substituted into transmembrane helices 1, 3 and 5, J. Biol. Chem. 282 (2007) 9001–9007.
[25] P.R. Steed, R.H. Fillingame, Subunit *a* facilitates aqueous access to a membrane-embedded region of subunit *c* in *Escherichia coli* ATP synthase, J. Biol. Chem. 283 (2008) 12365–12372.
[26] P.R. Steed, R.H. Fillingame, Aqueous accessibility to the transmembrane regions of subunit *c* of the *Escherichia coli* F_1F_0 ATP synthase, J. Biol. Chem. 284 (2009) 23243–23250.
[27] H. Gohlke, D. Schlieper, G. Groth, Resolving the negative potential (n-side) water-accessible proton pathway of F-type ATP synthase by molecular dynamics simulations, J. Biol. Chem. 287 (2012) 36536–36543.
[28] M.G. Duser, N. Zarrabi, D.J. Cipriano, S. Ernst, G.D. Glick, S.D. Dunn, M. Borsch, 36° step size of proton-driven *c*-ring rotation in F_oF_1-ATP synthase, EMBO J. 28 (2009) 2689–2696.
[29] R.R. Ishmukhametov, T. Horning, D. Spetzler, W.D. Frasch, Direct observation of stepped proteolipid ring rotation in *E. coli* F_oF_1-ATP synthase, EMBO J. 29 (2010) 3911–3923.
[30] H. Sielaff, M. Borsch, Twisting and subunit rotation in single F_0F_1-ATP synthase, Philos. Trans. R. Soc. B 368 (2012) 20120024.
[31] P.E. Hartzog, B.D. Cain, J. Biol. Chem. 269 (1994) 32313–32317.
[32] H. Dong, R.H. Fillingame, Chemical reactivities of cysteine substitutions in subunit *a* of ATP synthase define residues gating H^+-transport from each side of the membrane, J. Biol. Chem. 285 (2010) 39811–39818.
[33] K.J. Moore, R.H. Fillingame, Obstruction of transmembrane helical movements in subunit *a* blocks proton pumping by F_1F_o ATP synthase, J. Biol. Chem. 288 (2013) 25535–25541.
[34] K.J. Moore, C.M. Angevine, O.D. Vincent, B.E. Schwem, R.H. Fillingame, The cytoplasmic loops of subunit *a* of *Escherichia coli* ATP synthase may participate in the proton translocating mechanism, J. Biol. Chem. 283 (2008) 13044–13052.
[35] J. Symersky, V. Pagadala, D. Osowski, A. Krah, T. Meier, J.D. Faraldo-Gomez, D.M. Mueller, Structure of the c_{10} ring of the yeast mitochondrial ATP synthase in the open conformation, Nat. Struct. Mol. Biol. 19 (2012) 485–492.
[36] P.R. Steed, R.H. Fillingame, Residues in the polar loop of subunit *c* in Escherichia coli ATP synthase function in gating proton transport to the cytoplasm, J. Biol. Chem. 289 (2014) 2127–2138.
[37] D. Zhang, S.B. Vik, Close proximity of a cytoplasmic loop of subunit *a* with *c* subunits of the ATP synthase from *Escherichia coli*, J. Biol. Chem. 278 (2003) 12319–12324.
[38] W. Junge, H. Sielaff, S. Engelbrecht, Torque generation and elastic power transmission in the rotary F_0F_1-ATPase, Nature 459 (2009) 364–370